Pergamon

Cement and Concrete Research, Vol. 26, No. 12, pp. 1779-1787, 1996

0008-8846/96 $15.00 + .00

PII S0008-8846(96)00175-5

PRACTICAL EVALUATION OF RESISTIVITY OF CONCRETE IN TEST CYLINDERS USING A WENNER ARRAY PROBE

W. Morris, E.I. Moreno* and A.A. Sagüés
Department of Civil and Environmental Engineering
University of South Florida
Tampa, FL 33620 - U.S.A.
*Permanent affiliation: CINVESTAV-Mérida Unit, México

(Refereed)
(Received December 20, 1995; in final form October 16, 1996)

ABSTRACT

Cell constant correction values (K) for concrete resistivity measurements on cylindrical test samples performed with the four-point Wenner array probe technique are presented. Specimens dimensions correspond to standard cylinder sizes used for compressive strength or rapid chloride permeability tests, as well as typical concrete core sizes. The values of K were determined experimentally and numerically, by means of Finite Element (FE) simulation. The effect of different maximum aggregate sizes and aggregate types on the variability of the resistivity readings was evaluated. Cell constant correction values are given to allow quick determination of concrete resistivity. *Copyright © 1996 Elsevier Science Ltd.*

Introduction

The electric resistivity of water-saturated concrete is being increasingly used to indirectly evaluate concrete characteristics such as chloride ion diffusivity, permeability, and properties of the pore water solution [1-5]. The resistivity of concrete in service is an indicator of the possible extent of corrosion macrocell currents [6-9] and an important parameter in cathodic protection design [10]. Care must be exercised in relating electric properties of the concrete to other quality performance indicators [11-13]. However, the non-destructive nature, speed, and ease of conducting resistivity measurements make them an attractive addition to the battery of tests that can be performed to characterize concrete.

It is often necessary to measure the resistivity of concrete samples in the form of standard strength test cylinders, drilled cores, or slices cut out of those samples. In principle, the measurement could be made by placing flat electrodes on each end of the cylinder or slice, and by measuring the potential drop P between the electrodes when a current I is circulated [14]. The measurement requires alternating current to avoid excessive polarization of the electrodes [4,5]; P and I are normally determined as a.c. amplitudes (or equivalent magnitudes) using moderate frequencies. The resistivity ρ of the concrete can then be obtained by the following formula:

$$\rho = \frac{\pi d^2}{4L}\frac{P}{I} \tag{1}$$

in which L is the length of the cylinder, and d its diameter. The measurement is complicated by the need for effective and uniform electrical contacts between the end electrodes and the surface of the concrete, which may require very flat cylinder end surfaces, flexible electrodes or similar arrangements. To further reduce errors due to localized potential drops at the current insertion interfaces, it may become necessary to use a set of two independent potential measurement electrodes placed at the ends of the cylinder, but separate from the current delivery electrodes (four-electrode configuration) [15]. Experience at this laboratory has shown that implementing those procedures in large numbers of specimens can be highly time consuming. This is specially so when testing field-extracted cores of variable length which have an irregular broken end.

A convenient alternative to employing carefully constructed external electrodes is to use ready made, commonly available four-point Wenner probe resistivity meters [16-18]. These meters use a probe with four terminals set up in a linear array with a distance a between consecutive points of the array. The two outer points are the current insertion and removal points, whereas the two center points are the potential measurement points. The probe is made to touch the external concrete surface, while an electronic control unit circulates the test current and measures the potential. If P is the difference in potential between the potential points, and I is the current when the probe is in contact with the face of a semi-infinite uniform body, the resistivity of the body material is given by

$$\rho = 2\pi\, a\, \frac{P}{I} \tag{2}$$

In practice, the probe is in contact with bodies of finite dimensions. Calling P' and I' the potential and current values obtained when the probe is applied to a finite body, the apparent value ρ_{app} of the resistivity (which is the value shown in the display screen of commercial probes) is given by:

$$\rho_{app} = 2\pi\, a\, \frac{P'}{I'} \tag{3}$$

If the probe is applied to a wide concrete slab with thickness $\gg a$ and there is no interference from the reinforcing steel [6], then $\rho_{app} \simeq \rho$. For smaller bodies such as the concrete cylinders, a cell constant correction K can be defined such that,

$$\rho = \frac{\rho_{app}}{K} \tag{4}$$

where K is a function of the inter-probe distance a and the geometry of the concrete body tested.

The Wenner array probes can be used quickly and with virtually no special specimen preparation or need for custom-made electrodes. Thus, concrete resistivity measurements could be conducted in a convenient and quick fashion if the appropriate cell constants were known for common cylinder and probe test configurations. This paper briefly presents values of cell constant corrections for such purpose.

Procedure

Two types of test configurations were assumed. The first one consisted in placing the test point array longitudinally centered on the side of a test cylinder. The second configuration considered the test points centered on one of the end faces of the cylinder. This second configuration is convenient for cylinder slices such as those used in the AASHTO rapid chloride permeability test [19], as well as test cylinders that are still inside a curing mold with one end exposed.

The cell constant correction values were determined experimentally for selected cases, and by means of finite element (FE) simulations to cover a wider range of situations. The experimental method used empirical correlations between measurements with water-filled concrete-test-cylinder plastic molds and independent water resistivity measurements. The test cylinder mold sizes tested were 2, 3, 4, and 6 in. (5.08, 7.62, 10.2, and 15.2 cm) in diameter. Sets of four metallic electrodes (plated steel screws, 3 mm in diameter) where inserted flush with the inner diameter, leaving a 1 in. (2.54 cm) separation in-between them to establish the contacts with the tips of the Wenner probe or directly with the current source/potential measuring device. The liquid resistivity was measured with a standard test cell of the type used for soil resistivity measurements and a Nilsson model 400 soil resistivity meter [20]. Multiple tests were performed using water with resistivities that were in the 2,000 Ωcm to 10,000 Ωcm

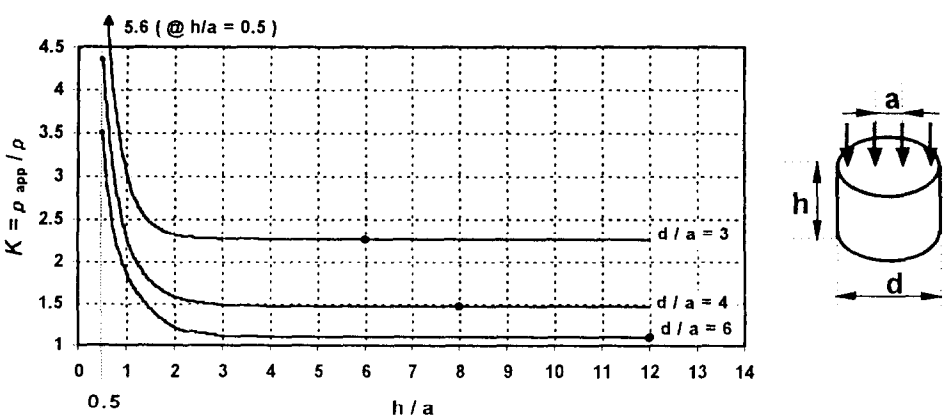

FIG. 1.

Cell constant correction to determine the concrete resistivity for the centered end face configuration. The circles ($K \sim 2.26$, $K \sim 1.47$ and $K \sim 1.09$) correspond to standard test cylinder sizes and $a = 1$ in. (2.54 cm).

TABLE 1

Mix Design of Samples Tested for Examining Variability of Results

Specimen	Type of Aggregate	Max. Agg. Size	W/C [+]	Cement Type	% of Fly Ash [++]
1	Limestone (L)	3/8 in. (0.95 cm)	0.37	I	0
2	River rock (R)	3/8 in. (0.95 cm)	0.37	I	20
3	Limestone (L)	3/4 in. (1.9 cm)	0.37 *	II *	20 *

* Field extracted core, 10 years old, nominal mix design.

[+] Water to total cementitious content ratio.

[++] % of total cementitious content, which was 444 kg/m^3.

range obtained by mixing tap water with distilled water in the appropriate proportions. The measurements of apparent resistivity on the cylinder were conducted with either a CNS RM MKII resistivity meter (trapezoidal wave a.c., ~13 Hz) which has a Wenner probe provided with wet wooden dowel tips to make contact, or with a Nilsson model 400 soil resistivity meter (square wave a.c., ~97 Hz) directly wired to the metallic screws. Both devices provided essentially the same results.

The FE simulations were performed using an ALGOR FE commercial package. Typical computations where performed using 3-D model, constructed with 8-node isoparametric brick elements. The total number of elements of each model varied from 800 to 1200 depending on the model dimensions. A denser mesh of elements was implemented where the current input condition was applied. In all cases a quarter of the total modeled volume was considered, taking advantage of the system symmetry.

A brief evaluation of the influence of the concrete aggregate size and type on the variability of the resistivity results was also conducted. A total of 20 measurements were performed at different radial positions on each cylindrical concrete specimen, following the measurement configuration shown in Figure 1. For each measurement the Wenner probe was centered over the longitudinal axis of the cylinder. In all the specimens, a cut surface was tested. Before taking the measurements, the specimens were kept in a 100% relative humidity chamber until constant weight (ca. 20 days). The specimens dimensions were 4 in. (10.2 cm) in diameter and 4 in. (10.2 cm) long. The inter-probe spacing used was 1 in. (2.54 cm). For these conditions, (h/a = 4 and d/a = 4) Figure 1 shows that $K \sim 1.48$. The specimens represented two different maximum aggregate sizes (3/4 in. (1.9 cm) and 3/8 in. (0.95 cm)) as well as two different types of aggregate (limestone and river rock). Table 1 shows the mix designs of the concrete cylinders tested.

Results

Figures 1 and 2 show the model-calculated cell constant correction for the two types of configuration considered as a function of the cylinder dimensions and the inter-probe distance. The results corresponding to standard cylinder sizes (3, 4 and 6 in. (7.62, 10.2, and 15.2 cm) in diameter), when measured with an inter-probe distance of 1 in. (2.54 cm), are indicated with circles in the curves for $d/a = 3$, 4, and 6 respectively.

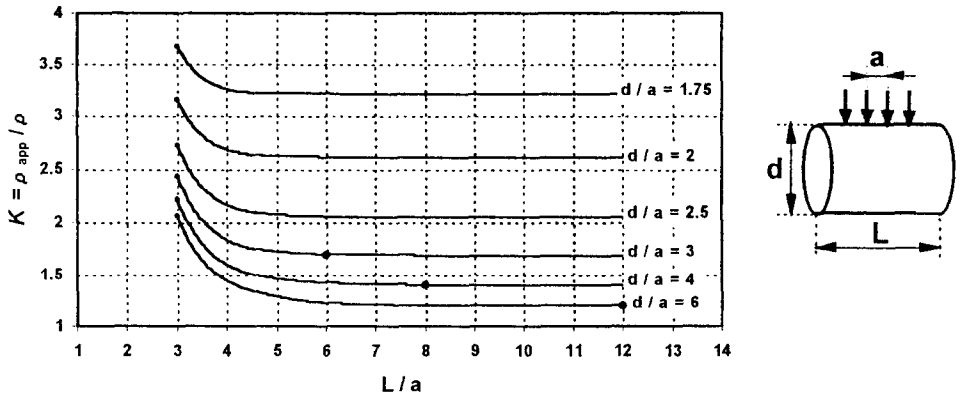

FIG. 2.

Cell constant correction to determine the concrete resistivity for the centered longitudinal measuring configuration. The circles ($K \sim 1.73$, $K \sim 1.41$ and $K \sim 1.20$) correspond to standard cylinder sizes and $a = 1$ in. (2.54 cm).

A longitudinal cross section illustration of the FE mesh and the corresponding modulus current density distribution isolines when performing the lengthwise four-point measurement is shown in Figure 3. The values of current densities indicated in the figure are given in A/cm^2, and correspond to a current $I = 3.92 \cdot 10^{-3}$ A, and a difference of potential $P = 0.69$ V between the potential points, when an assumed resistivity of 2,000 Ωcm is considered.

The correlation between the experimental and modeled values of the cell constant correction K calculated for the different cylinder sizes and measurement configurations is shown in Figure

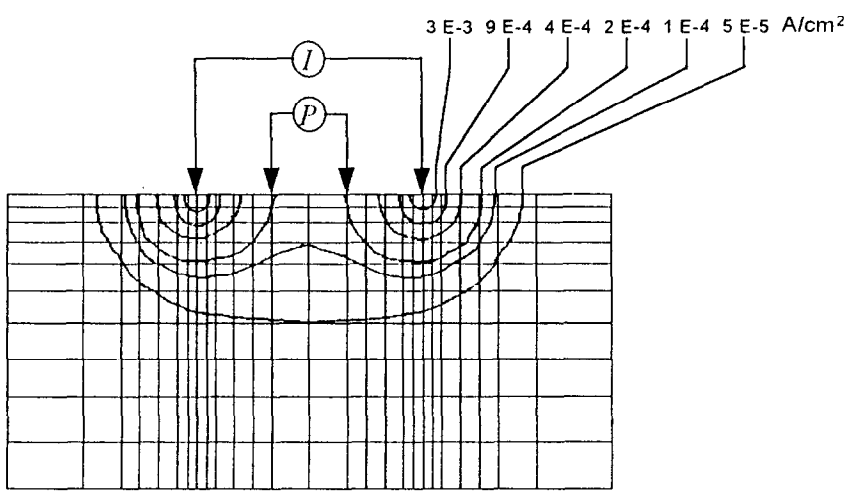

FIG. 3.

FE mesh and current density distribution, indicating the current insertion and potential measurement points. Case in which $L/a = 8$, $d/a = 4$, and $a = 2.54$ cm. The isocurrent density lines correspond to an assumed $\rho = 2{,}000$ Ωcm, when $I = 3.92 \cdot 10^{-3}$ A, and $P = 0.69$ V.

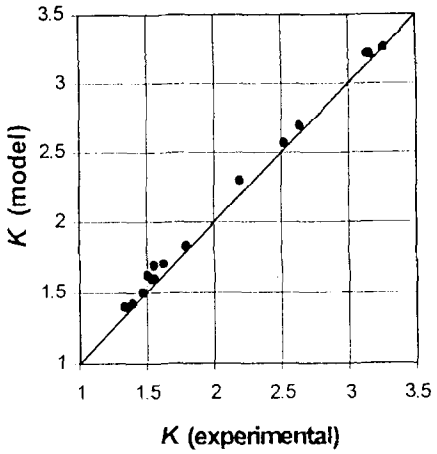

FIG. 4.
Correlation between experimental and modeled results (solid line for ideal 1:1 ratio).

4. Direct resistivity tests of 9 actual concrete cylinders fitted with flat end electrodes were also conducted using a soil resistivity meter and then applying Eq. (1). The results deviated <6%, on average, from measurements conducted using a Wenner array and applying the correction per Figure 2.

The effect of the aggregate size and type on the variability of the resistivity readings tested on the three concrete specimens is exemplified by the results presented in Table 2. The CNS probe was used for these tests. The values of standard deviation were obtained from a set of 20 readings performed on each specimen and are based on the values of apparent resistivities. Notice the influence of fly ash in the resistivity measurements when comparing specimen 1 and 2, and the influence of aging when comparing specimen 2 and 3.

TABLE 2

Variability of Resistivity Readings with the Aggregate Size

Specimen	Maximum Aggregate Size and Type	ρ_{app}* (kΩ cm)	S=Standard Deviation of ρ_{app} (kΩ cm)	Coefficient of variation $\frac{S}{\rho_{app}} \times 100$	$\rho = \frac{\rho_{app}}{K}$ (kΩ cm)
1	3/8 in. (0.95 cm) (L)	9.0	0.6	6.7 %	6.1
2	3/8 in. (0.95 cm) (R)	20.3	0.9	4.4 %	13.7
3	3/4 in. (1.9 cm) (L)	41.9	4.5	11 %	28.3

* Average of 20 measurements.

The cumulative percentage readings as a function of the ratio of the measured to average apparent resistivity values are shown in Figure 5. Tests performed using the probe arrangement of Figure 2 gave essentially the same results.

Discussion

Equations 1-4 assume that the concrete behaves as a homogenous medium, which it is not. Application of these formulas implies, instead, an averaging of the material resistivity over the volume sampled. As can be observed in Figure 3, the current distribution when using a Wenner probe is highly non-uniform, and the resistivity measurement tends to be representative of the concrete region located roughly between the two center potential probes, extending into the concrete by a length on the order of the inter probe distance. As the readings show variability (increasing with the aggregate size, Figure 5), it is desirable to perform multiple measurements at different tangential locations on the cylinder surface, or rotating the probe array on the cylinder face. This can be made easily and results then averaged. Since each resistivity reading in nearly instantaneous and no custom fitting of the specimen is needed, large numbers of specimens can be characterized in a short time, even when several readings per specimen are made for averaging.

As shown in Table 2 and Figure 5, the coefficient of variation of a series of individual readings was on the order of 4 to 11% of the average value for typical specimen conditions. Although 20 tests were made in each series to better reveal statistical patterns, averaging of a small number of measurements (e.g. 5) in those specimens should provide enough statistical significance for most practical purposes. The variability was greater on the specimen with the larger maximum aggregate size. The specimens that had the same maximum aggregate size but were made with different aggregate type showed comparable values of standard deviation. Statistics tests of the type shown here should be performed before evaluating a series of unknown specimens.

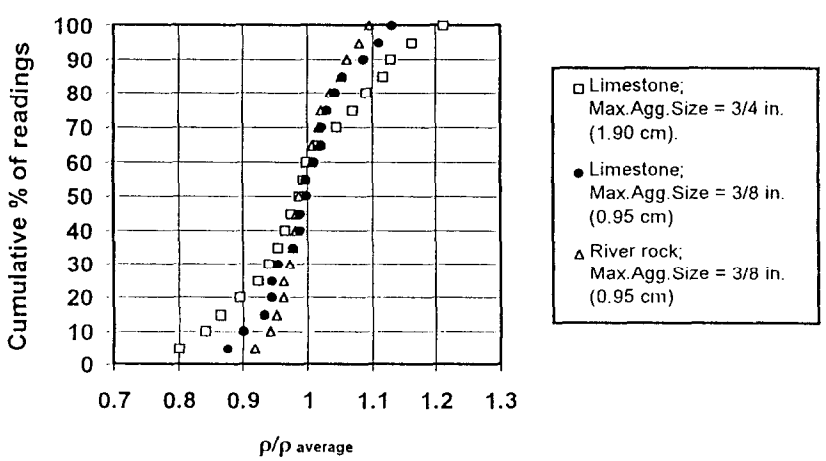

FIG. 5.
Influence of the aggregate size and type on the variability of the resistivity readings.

The curves in Figures 1 and 2 address a wide variety of h/a and L/a values. For specimens having ideal cylindrical shape, less variability in repeated tests is expected when using the largest practical value of a, since as indicated above the volume averaging effect is better. This averaging minimizes also the effects from the presence of transition zones from the surface into the bulk (such as those resulting from laitance on troweled surfaces, or molded surfaces where the coarse aggregate distribution varies from the bulk). Tests having specimens with cut surfaces, as in cored cylinders or cut cylinder ends, should show less systematic effects from transition zones.

If a specimen has an irregular broken end (as in filed extracted cores) and the configuration in Figure 2 is used, then a should be limited to avoid inaccuracy due to the irregular end. Figure 2 shows that the cell constant correction becomes insensitive to L/a at large values of L/a. The curves can then be used as a guide in choosing a value of a small enough that the uncertainty in L/a caused by the irregular end yields a tolerable error in K. A similar sensitivity analysis can be applied to the test configuration in Figure 1 when having shape irregularities at the opposite end.

Specimens presenting carbonated layers, uneven consolidation or other systematic non-uniformity may deviate considerably from the assumptions used in these calculations [16], and might require a specialized treatment to define an effective average concrete resistivity. This study addressed only the predominantly resistive character of the concrete impedance as observed at moderate test frequencies. Concrete behavior over a wide frequency range may vary and the entire electromagnetic response of the material should be considered in that case [5].

Conclusions

1) The concrete resistivity of test cylinders can be quickly determined with a four-point Wenner array probe and the application of a cell constant correction K. The value of K was computed as a function of the dimensions of the tested cylinder, the measurement configuration type, and the inter-probe distance a.
2) The resistivity readings using typical probe spacing and concrete specimens dimensions show moderate variability from coarse aggregate distribution effects. Averaging of multiple readings with distinct but equivalent probe placement should be conducted to obtain a better resistivity estimate. Specimens with systematic heterogeneity or wide frequency impedance behavior determination require specialized analysis.

References

1. N.S. Berke and M.C. Hicks, in Corrosion Forms and Control for Infrastructure, ASTM STP 1137, p. 207, V. Chaker, Ed., American Society for Testing and Materials, Philadelphia, 1992.
2. C. Andrade, M.A. Sanjuán, and C. Alonso, 'Measurement of Chloride Diffusion Coefficient from Migration Tests', CORROSION/93, Paper No. 319, NACE, 1993.
3. C. Andrade, C. Alonso, and S. Goñi, in Concrete 2000, R.K. Dhir and M.R. Jones, Eds., p. 1640, E. & F.N. Spon, London, 1993.
4. G. Monfore, J. PCA Res. Develop. Lab., 10, 35 (1968).
5. B.J. Christensen, R.T. Coverdale, R.A. Olson, S.J. Ford, E.J. Garboczi, H.M. Jennings, and T.O. Mason, J. Am. Ceram. Soc., 77, 2789 (1994).

6. S.G. Millard, J.A. Harrison, and A.J. Edwards, Br. J. Non-Destr. Test., 31, 617 (1989).
7. A.A. Sagüés and S.C. Kranc, Corrosion, 50, 50 (1994).
8. R.F. Stratfull, Mater. Prot., 7, No. 3, 29 (1968).
9. R. Brownie, in Performance of Concrete in Marine Environment, ACI SP-65, p. 169, V.M. Malhotra, Ed., American Concrete Institute, Detroit, 1980.
10. A.A. Sagüés and R.G. Powers,Sprayed Zinc Galvanic Anodes for Concrete Marine Bridges Substructures, SHRP-S-405, National Research Council, Washington, DC, 1994.
11. D.W. Pfeifer, D.B. McDonald, and P.D. Krauss, PCI Journal, 39, No. 1, 38 (1994).
12. D. McDonald and D.W. Pfeifer, ACI Mat. J., 91, 636 (1994).
13. H. Arup, B. Sørensen, J. Frederiksen, and N. Thaulow, 'The Rapid Chloride Permeation Test-An Assessment', CORROSION/93, Paper No. 334, NACE, 1993.
14. W.J. McCarter, M.C. Forde, and H.W. Whittington, Proc. Instn. Civ. Engrs., Pt. 2, 71, 107 (1981).
15. J.W. Mayer and S.S. Law, Electronic Materials Science for integrated circuits in Si and GaAs, p. 32, Macmillan Publishing Company, New York, (1990).
16. W.J. McCarter and A. Barclay, Cement and Concrete Research, 23,1178, (1993).
17. S.G. Millard, M.H. Ghassemi, J.H. Bungey, and M.I. Jafar, in Corrosion of Reinforcement in Concrete, p. 303, C.L. Page, K.W.J. Treadway, and P.B. Bamforth, Eds., Elsevier Appl. Science, London, 1990.
18. A.J. Ewins, Br. J. Non-Destr. Test., 32, 120 (1990).
19. D. Whiting, Public Roads, 43, 101 (1981).
20. ASTM G-57, Standard Method for Field Measurement of Soil Resistivity Using the Wenner Four-Electrodes Method, American Society for Testing and Materials, Philadelphia, 1984.